Molecular Crystals and Liquid Crystals
Publication details, including instructions for authors and subscription information:
http://www.tandfonline.com/loi/gmcl16

Structural Study of the Crystal and Mesomorphic States of trans, trans-4′- Butyl-bicyclohexyl-4-Carboxylic Acid (ZLI 1756)

S. Barocci [c] , E. Foresti [a] , S. Melone [c] , S. Ottani [b] & G. Torquati [c]

[a] Facoltà di Chimica Industriale, Viale Risorgimento, Bologna, 4, 40136, Italy

[b] Centro di Studio per la Fisica delle Macromolecole del C.N.R., Istituto di Chimica "G. Ciamician" Università di Bologna, Via Selmi, Bologna, 2-40126, Italy

[c] Facoltà di Ingegneria, Università degli Studi di Ancona, Ancona, Italy

Version of record first published: 20 Apr 2011.

To cite this article: S. Barocci , E. Foresti , S. Melone , S. Ottani & G. Torquati (1984): Structural Study of the Crystal and Mesomorphic States of trans, trans-4′- Butyl-bicyclohexyl-4-Carboxylic Acid (ZLI 1756), Molecular Crystals and Liquid Crystals, 108:3-4, 255-267

To link to this article: http://dx.doi.org/10.1080/00268948408078678

Mol. Cryst. Liq. Cryst., 1984, Vol. 108, pp. 255–267
0026-8941/84/1084–0255/$18.50/0

Printed in the United States of America

Structural Study of the Crystal and Mesomorphic States of trans,trans-4′-Butyl-bicyclohexyl-4-Carboxylic Acid (ZLI 1756)

S. BAROCCI,§ E. FORESTI,† S. MELONE,§ S. OTTANI‡ and G. TORQUATI §

(*Received September 26, 1983; in final form January 9, 1984*)

The crystal structure at room temperature and the phase transitions of the title compound (ZLI 1756, Merck, Darmstadt), whose smectic B phase displays catalytic effects on the monomolecular rearrangements of terpene derivatives, have been investigated. The compound changes on heating from a crystalline phase stable at room temperature to another solid phase, then to a smectic B phase and later to a nematic phase. The crystal structure has been determined at room temperature by direct methods and refined by least-squares methods to $R = 0.072$ for 2339 observed reflections. The compound crystallizes in space group $P2_1/c$ with $a = 21.934(5)$, $b = 5.384(2)$, $c = 27.681(7)$ Å, $\beta = 97.35(3)°$ and $Z = 8$. The molecules are arranged as hydrogen-bonded dimers. The four cyclohexyl rings have the chair conformation and the butyl chains have the *trans*-planar conformation. The packing is layer-like with the molecules inclined to the layers, which are the (100) planes. The chain-chain interactions occur at the aliphatic surface parallel to the layers. The inclination of the molecules relative to the layers disappears at the change from the solid to the smectic B phase, but the dimeric arrangement remains in this phase too.

INTRODUCTION

It has been shown that smectic solvents are able to exert stereochemical and catalytic effects on reactions with severe orientational de-

†Facoltà di Chimica Industriale, Viale Risorgimento 4, 40136 Bologna (Italy).
‡Centro di Studio per la Fisica delle Macromolecole del C.N.R. Istituto di Chimica "G. Ciamician" Università di Bologna, Via Selmi 2—40126–Bologna (Italy).
§Facoltà di Ingegneria, Università degli Studi di Ancona, Ancona (Italy).

mands in the transition state, because of the enforced anisotropy of all diffusions of the reactant molecules by the ordered solvent structure.[1-7]

Recently the smectic B phases of alkyl-cyclohexyl and alkyl-bicyclohexyl-carboxylic acids and their mixtures with *p*-toluic acid have been used to promote the monomolecular rearrangements of limonene and linallol.[7] One of the mesomorphic media used in these catalytic studies was the smectic B phase of *trans,trans*-4′-butyl-bicyclohexyl-4-carboxylic acid (ZLI 1756, Merck, Darmstadt). Since knowledge of the structure of this substance could be important in order to achieve a better insight of the constraints exerted by the solvent structure on the conformations and the translational diffusions of the guest reactant molecules, we report here the results of an investigation of the crystal structure at room temperature and of the phase transitions of ZLI 1756 by X-ray diffraction.

1. CRYSTAL STRUCTURE

1.1. Crystal Data

$C_{17}O_2H_{30}$, $M = 266.4$, Monoclinic, $a = 21.934(5)$, $b = 5.384(2)$, $c = 27.681(7)$ Å, $\beta = 97.35(3)°$, $U = 3{,}342(2)$Å^3, $Z = 8$, 2 independent molecules (A) and (B), $Dc = 1.06$ g cm^{-3}, space group $P2_1/c$ (no. 14), $F(000) = 1184$, Cu − Kα radiation, $\lambda = 1.5418$ Å, μ (Cu − Kα) = 4.65 cm^{-1}.

1.2 X-ray analysis

Precise unit cell dimensions were determined by a least-squares treatment of 25 independent 2θ values. Diffraction intensities were measured in two octants of the reciprocal lattice in the range $3 < \theta < 60°$ by the $\theta - 2\theta$ method, using a single-crystal Siemens AED automated diffractometer. The scan speed and width were 3–12°/min and $(\theta - 0.5) + [\theta + (0.5 + \Delta\theta)]$, where $\Delta\theta = tg\theta(\lambda\alpha_2 - \lambda\alpha_1)/\lambda$, respectively. No appreciable changes in intensity were observed during data collection. Of 5525 independent reflections, 2339 having $I > 2\sigma(I)$ were considered observed and used in the analysis. Intensity data were corrected for Lorentzian and polarization effects, but not for absorption.

The structure was solved by direct methods and refined by least-squares methods with the SHELX[8] crystallographic program system; the first E map indicated positions for all the non-hydrogen atoms (except one of the butyl chains), which were subsequently identified

from a difference map. The structure was refined by least-squares calculations and, due to the high number of atoms, the normal matrix was divided into two blocks of nineteen atoms each. The non-hydrogen atoms were treated anisotropically. The hydrogen atoms were geometrically positioned (assuming C—H = 1.08 Å) and included in structure factor calculations with isotropic temperature factors equal for all, but their parameters were not varied. The weighting scheme

TABLE I

Atomic coordinates ($\times 10^4$) with estimated standard deviations in parentheses

	x/a	*y/b*	*z/c*
C(1A)	4577(3)	−3653(17)	3290(3)
C(2A)	4410(3)	−1211(17)	3040(3)
C(3A)	3959(3)	−1506(15)	2574(2)
C(4A)	3827(3)	991(15)	2319(2)
C(5A)	3405(3)	795(15)	1825(2)
C(6A)	2747(3)	169(16)	1883(2)
C(7A)	2321(3)	146(15)	1395(2)
C(8A)	2341(3)	2565(14)	1108(2)
C(9A)	3005(3)	3150(17)	1061(2)
C(10A)	3418(3)	3212(17)	1549(3)
C(11A)	1934(3)	2449(14)	616(2)
C(12A)	1246(3)	1958(16)	670(2)
C(13A)	837(3)	1836(16)	177(2)
C(14A)	887(3)	4268(15)	−107(2)
C(15A)	1559(3)	4790(16)	−169(2)
C(16A)	1968(3)	4826(16)	322(2)
C(17A)	486(3)	4221(18)	−595(2)
O(1A)	83(2)	2697(11)	−696(2)
O(2A)	594(2)	5942(13)	−892(2)
C(1B)	−4639(3)	1321(16)	−5756(3)
C(2B)	−4400(3)	3658(16)	−5515(2)
C(3B)	−3956(3)	3237(14)	−5048(2)
C(4B)	−3767(3)	5632(14)	−4784(2)
C(5B)	−3348(2)	5210(13)	−4297(2)
C(6B)	−3299(3)	7595(14)	−3994(2)
C(7B)	−2895(3)	7254(13)	−3513(2)
C(8B)	−2244(3)	6405(13)	−3584(2)
C(9B)	−2278(3)	4065(14)	−3891(2)
C(10B)	−2708(2)	4376(14)	−4378(2)
C(11B)	−1810(2)	6222(14)	−3103(2)
C(12B)	−1147(3)	5993(18)	−3172(2)
C(13B)	−711(3)	6059(16)	−2688(2)
C(14B)	−899(3)	4111(15)	−2340(2)
C(15B)	−1562(3)	4378(17)	−2269(2)
C(16B)	−1985(3)	4306(16)	−2759(2)
C(17B)	−493(3)	4205(17)	−1847(2)
O(1B)	−100(2)	5788(10)	−1746(1)
O(2B)	−606(2)	2511(11)	−1550(2)

was $.91/[\sigma^2(F_0) + 0.08163\ F_0^2]$. The final agreement index was $R = 0.072$. The coordinates of all the refined atoms are reported in Table I.

Bond distances and angles are listed in Tables II and III respectively.

Thermal parameters and observed and calculated structure factors are available from the Authors on request.

TABLE II

Bond distances (Å) with estimated standard deviations in parentheses

C(1A)—C(2A)	1.508(13)
C(2A)—C(3A)	1.531(9)
C(3A)—C(4A)	1.529(11)
C(4A)—C(5A)	1.554(8)
C(5A)—C(6A)	1.510(9)
C(5A)—C(10A)	1.511(12)
C(6A)—C(7A)	1.539(9)
C(7A)—C(8A)	1.529(11)
C(8A)—C(9A)	1.512(9)
C(8A)—C(11A)	1.531(8)
C(9A)—C(10A)	1.528(9)
C(11A)—C(12A)	1.559(9)
C(11A)—C(16A)	1.524(11)
C(12A)—C(13A)	1.535(9)
C(13A)—C(14A)	1.538(11)
C(14A)—C(15A)	1.532(9)
C(14A)—C(17A)	1.514(8)
C(15A)—C(16A)	1.530(8)
C(17A)—O(1A)	1.211(10)
C(17A)—O(2A)	1.282(10)
C(1B)—C(2B)	1.487(11)
C(2B)—C(3B)	1.534(8)
C(3B)—C(4B)	1.514(10)
C(4B)—C(5B)	1.547(7)
C(5B)—C(6B)	1.530(10)
C(5B)—C(10B)	1.518(8)
C(6B)—C(7B)	1.514(8)
C(7B)—C(8B)	1.535(8)
C(8B)—C(9B)	1.516(10)
C(8B)—C(11B)	1.536(7)
C(9B)—C(10B)	1.553(7)
C(11B)—C(12B)	1.496(9)
C(11B)—C(16B)	1.487(10)
C(12B)—C(13B)	1.544(8)
C(13B)—C(14B)	1.515(10)
C(14B)—C(15B)	1.500(9)
C(14B)—C(17B)	1.533(8)
C(15B)—C(16B)	1.542(8)
C(17B)—O(1B)	1.219(9)
C(17B)—O(2B)	1.274(10)

TABLE III

Bond angles (°) with estimated standard deviation in parentheses

C(1A)—C(2A)—C(3A)	112.9(7)
C(2A)—C(3A)—C(4A)	111.2(6)
C(3A)—C(4A)—C(5A)	113.8(6)
C(4A)—C(5A)—C(6A)	113.1(5)
C(4A)—C(5A)—C(10A)	109.8(6)
C(6A)—C(5A)—C(10A)	109.1(6)
C(5A)—C(6A)—C(7A)	112.9(5)
C(6A)—C(7A)—C(8A)	113.2(6)
C(7A)—C(8A)—C(9A)	108.3(6)
C(7A)—C(8A)—C(11A)	112.1(6)
C(9A)—C(8A)—C(11A)	112.9(5)
C(8A)—C(9A)—C(10A)	113.4(5)
C(5A)—C(10A)—C(9A)	112.3(7)
C(8A)—C(11A)—C(12A)	112.6(5)
C(8A)—C(11A)—C(16A)	112.3(6)
C(12A)—C(11A)—C(16A)	107.8(5)
C(11A)—C(12A)—C(13A)	112.7(5)
C(12A)—C(13A)—C(14A)	110.3(6)
C(13A)—C(14A)—C(15A)	110.2(6)
C(13A)—C(14A)—C(17A)	111.7(6)
C(15A)—C(14A)—C(17A)	111.1(5)
C(14A)—C(15A)—C(16A)	111.4(5)
C(11A)—C(16A)—C(15A)	113.7(6)
C(14A)—C(17A)—O(1A)	122.7(7)
C(14A)—C(17A)—O(2A)	115.2(7)
O(1A)—C(17A)—O(2A)	122.1(6)
C(1B)—C(2B)—C(3B)	113.7(6)
C(2B)—C(3B)—C(4B)	112.7(6)
C(3B)—C(4B)—C(5B)	113.0(8)
C(4B)—C(5B)—C(6B)	110.3(5)
C(4B)—C(5B)—C(10B)	111.9(4)
C(6B)—C(5B)—C(10B)	109.2(5)
C(5B)—C(6B)—C(7B)	111.9(6)
C(6B)—C(7B)—C(8B)	112.0(5)
C(7B)—C(8B)—C(9B)	109.8(5)
C(7B)—C(8B)—C(11B)	113.1(5)
C(9B)—C(8B)—C(11B)	114.4(5)
C(8B)—C(9B)—C(10B)	112.3(6)
C(5B)—C(10B)—C(9B)	111.9(5)
C(8B)—C(11B)—C(12B)	113.6(5)
C(8B)—C(11B)—C(16B)	114.6(5)
C(12B)—C(11B)—C(16B)	111.0(6)
C(11B)—C(12B)—C(13B)	113.0(5)
C(12B)—C(13B)—C(14B)	110.3(6)
C(13B)—C(14B)—C(15B)	111.4(6)
C(13B)—C(14B)—C(17B)	111.6(6)
C(15B)—C(14B)—C(17B)	110.0(5)
C(14B)—C(15B)—C(16B)	111.5(5)
C(11B)—C(16B)—C(15B)	111.7(6)
C(14B)—C(17B)—O(1B)	122.7(7)
C(14B)—C(17B)—O(2B)	114.4(6)
O(1B)—C(17B)—O(2B)	122.9(5)

1.3. Description of the structure

The crystal is composed of pairs of molecules held together by hydrogen bonds between the carboxylic groups (Figure 1). The hydrogen bonds O(1A)—O(2B) and O(2A)—O(1B) are of length 2.640 and 2.664 Å, respectively. Relevant torsion angles are reported in Table IV. The four cyclohexyl rings have the chair form and the mean C—C bond length is 1.525 Å. The butyl chains have an all-*trans* planar conformation with normal bond distances and angles.

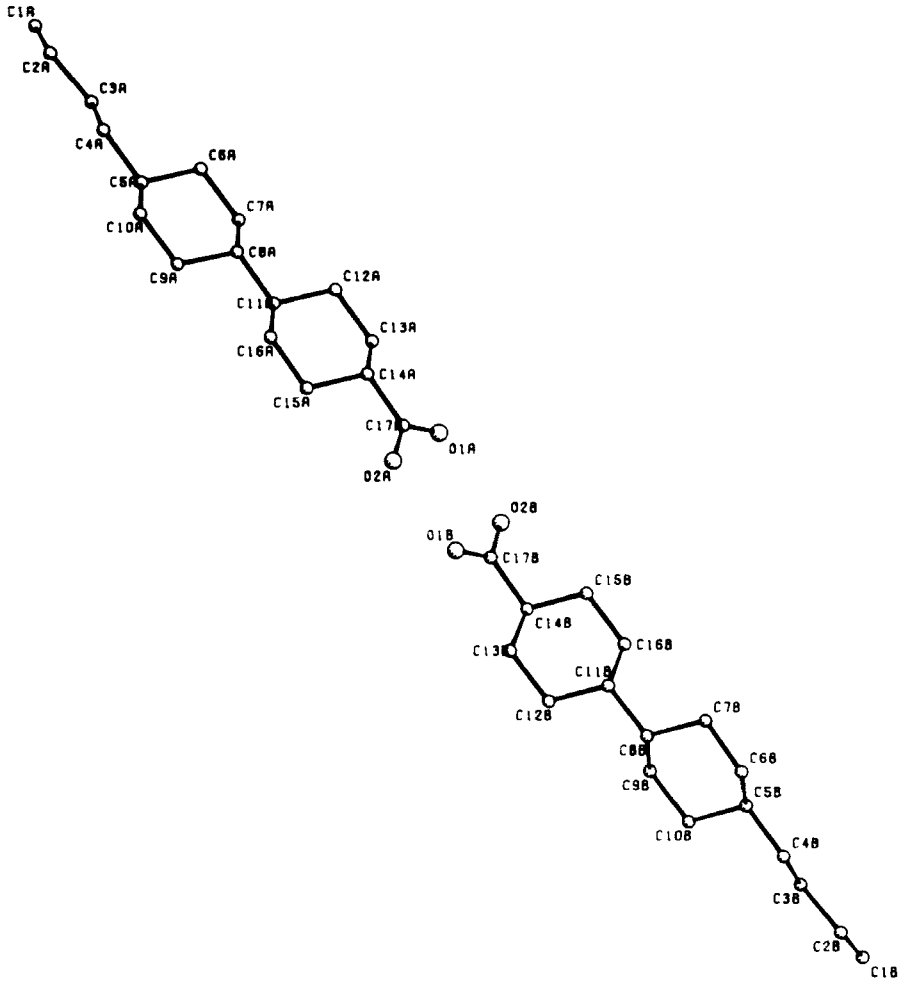

FIGURE 1 The hydrogen bonded dimer and numbering scheme in *b*-axis projection.

TABLE IV

Relevant torsion angles (°)

C(7A)—C(8A)—C(11A)—C(12A)	59.80
C(7A)—C(8A)—C(11A)—C(16A)	−178.22
C(9A)—C(8A)—C(11A)—C(12A)	−177.54
C(9A)—C(8A)—C(11A)—C(16A)	−55.56
C(13A)—C(14A)—C(17A)—O(1A)	14.85
C(13A)—C(14A)—C(17A)—O(2A)	−166.50
C(15A)—C(14A)—C(17A)—O(1A)	138.45
C(15A)—C(14A)—C(17A)—O(2A)	−42.91
C(7B)—C(8B)—C(11B)—C(12B)	−166.30
C(7B)—C(8B)—C(11B)—C(16B)	64.59
C(9B)—C(8B)—C(11B)—C(12B)	67.04
C(9B)—C(8B)—C(11B)—C(16B)	−62.07
C(13B)—C(14B)—C(17B)—O(1B)	4.89
C(13B)—C(14B)—C(17B)—O(2B)	−175.96
C(15B)—C(14B)—C(17B)—O(1B)	−119.30
C(15B)—C(14B)—C(17B)—O(2B)	59.85

The two crystallographically independent molecules assume different global conformations, the torsion angles around the C—C bond connecting the cyclohexyl rings being different. The distance between the two extreme methyl groups of the dimer is 30.25 Å.

The crystal packing (Figure 2) is characterized by hydrogen-bonded dimers which form stacks with a translation along the stacking axis (*b*-axis) of 5.38 Å. The packing is also layer-like with the molecules inclined to the layers, which are the (100) planes.

The chain-chain interactions between adjacent stacks occur at surfaces of aliphatic character parallel to the layers. The projection of the long molecular axis onto the (010) plane forms an angle of approximately 42° with the *c*-axis.

2. MESOMORPHIC STATES

X-ray diffraction investigations have been performed on the different phases exhibited by ZLI 1756 by successive heating and cooling of the sample. An Elliot toroidal X-ray camera was used with nickel-filtered CuK radiation ($\lambda = 1.542$ Å) from a Rigaku-Denki rotating anode generator. In addition a conventional X-ray powder diffractometer was used. The sample had a thickness of 1 mm and was held by two very thin Al sheets fixed to a circular hole in an Al matrix with a diameter of 8 mm. Heating was by a hot stage with a temperature control of ± 0.1°C.

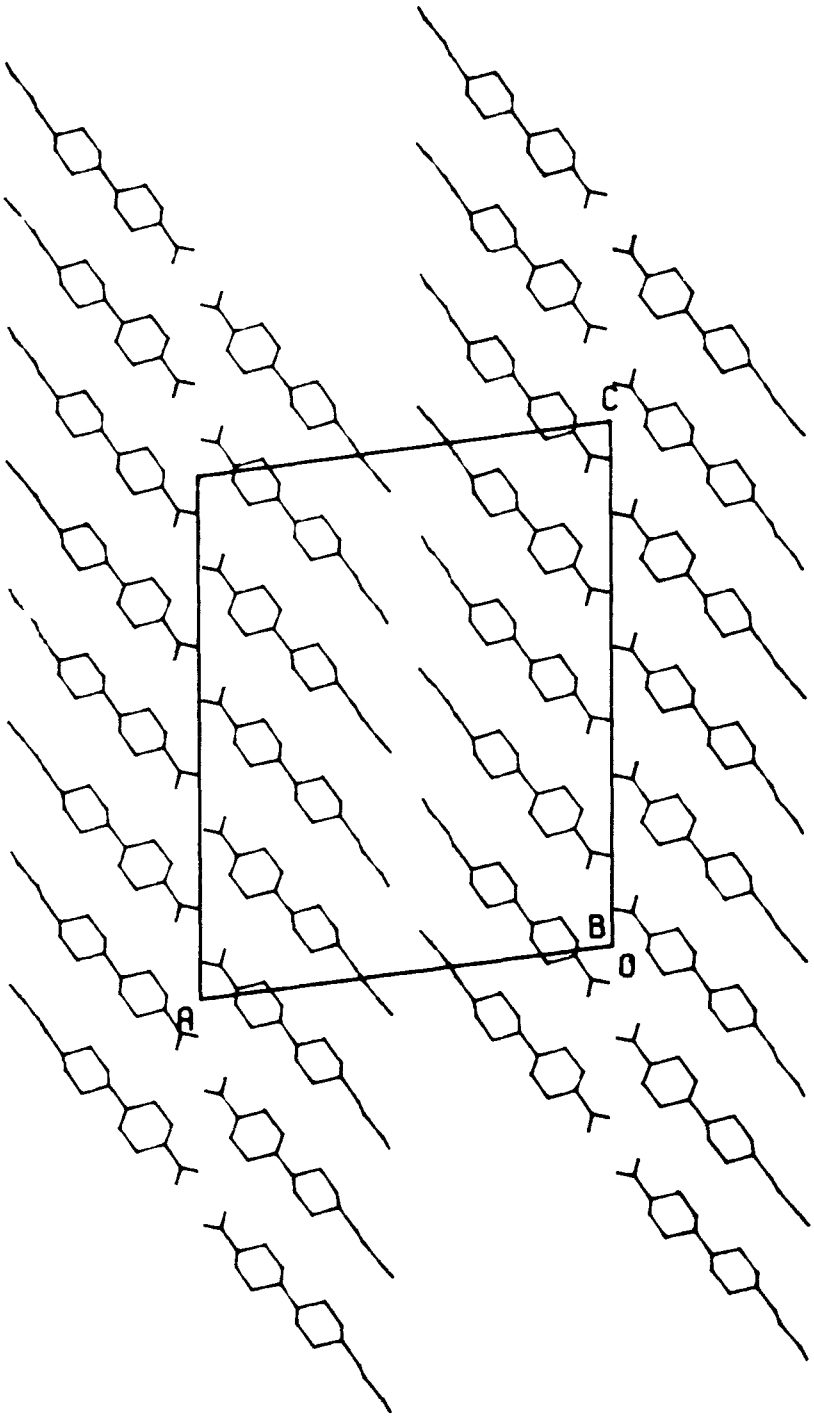

FIGURE 2 Molecular packing seen in *b*-axis projection.

We have obtained the following phase behaviour on heating:

$$K_2 \xrightarrow{36\,^\circ C} K_1 \xrightarrow{150\text{-}155\,^\circ C} S_B \xrightarrow{201\text{-}206.5\,^\circ C} N \xrightarrow{236\,^\circ C} I$$

and on cooling:

$$K_2 \xleftarrow[\text{at room temp.}]{\text{very slowly}} K_1 \xleftarrow{146\text{-}151\,^\circ C} S_B \xleftarrow{196\text{-}201\,^\circ C} N \xleftarrow{236\,^\circ C} I$$

where K_1 and K_2 represent two different solid phases.

A supercooling effect and, as specified below, a region of phase coexistence occur at the K_1–smectic B and smectic B–nematic phase transitions. A similar supercooling effect has already been observed at the similar solid–smectic H phase transition for TBBA[12].

The first transition occurs at 36 °C. The phase obtained at this temperature appears to be another solid phase. The diffraction patterns obtained respectively at 30 and 40 °C for the two solid phases (for technical details see ref. 7) are shown in Figure 3. The smectic B and nematic phases have already been investigated by X-ray diffraction, due to the important catalytic effect of the smectic B phase, and the structural results obtained are reported in ref. 7.

In this work, the study of the phase transitions K_1–smectic B and smectic B–nematic was performed. Figure 4 shows the results obtained at the K_1–smectic B phase transition. The diffraction peak associated with the solid phase K_1 progressively disappears as the

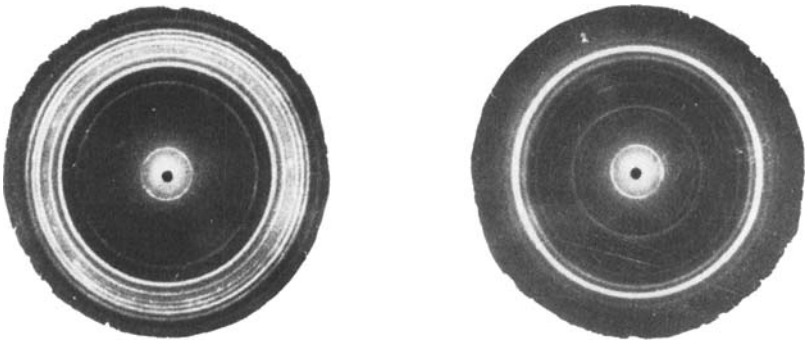

FIGURE 3 X-ray diffraction patterns from the K_2 (left side) and K_1 (right side) solid phases of ZLI 1756.

temperature is increased. Simultaneously the 100 peak associated with the smectic B phase progressively increases (Figure 4a). The two peak intensities are reported as a function of temperature in Figure 4b, after the smectic B 100 peak had been multiplied by an appropriate factor in order to display all the peak intensities on a single diagram.

Figure 4c reports the derivatives with respect to temperature of the intensities in Figure 4b. The full width (w) at half maximum is 2.4°.

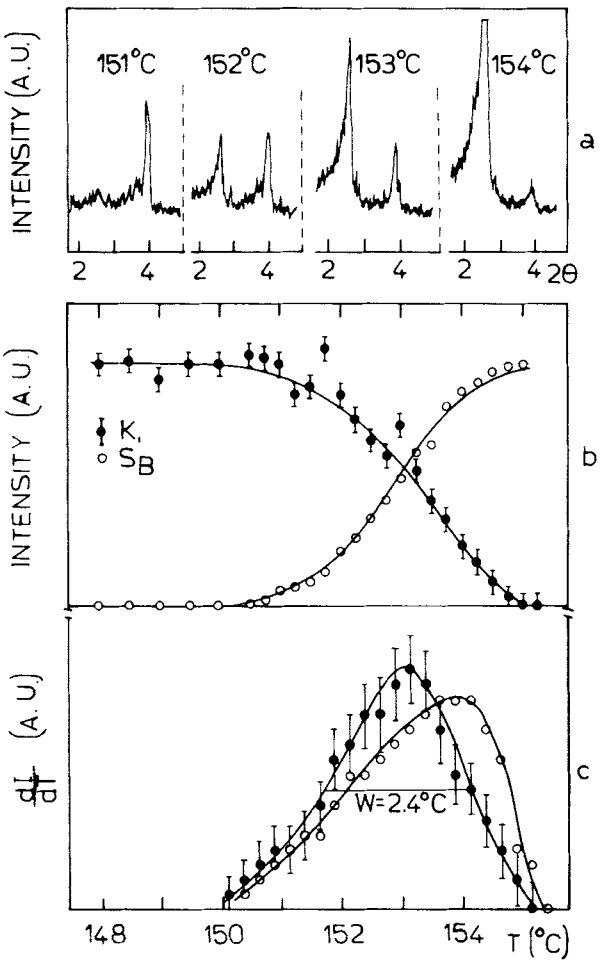

FIGURE 4 Solid K_1–S_B phase transition. *a*) Diffraction patterns at different temperatures. *b*) Bragg diffraction peak intensities *versus* temperature. *c*) Derivative of the Bragg diffraction peak intensities with respect to the temperature dI/dT. For clarity, the error bars are not given in the diagrams for the S_B phase.

In order to be sure that the observed phase coexistence is not due to a temperature gradient, the irradiated area was in one case greatly reduced: no change in data was observed. Moreover other reference compounds inserted in the same sample-holder showed, in the same temperature region, an abrupt phase transition occurring within 1°C. Decomposition of the sample can be excluded, as no change in the transition temperature after several heating cycles was obtained.

The observed phase coexistence is compatible with the results of ref. 13, where all phenomena related to pretransitional effects, premelting, and phase coexistence are extensively considered both experimentally and theoretically on the basis of the heterophase fluctuation theory of Frenkel[14].

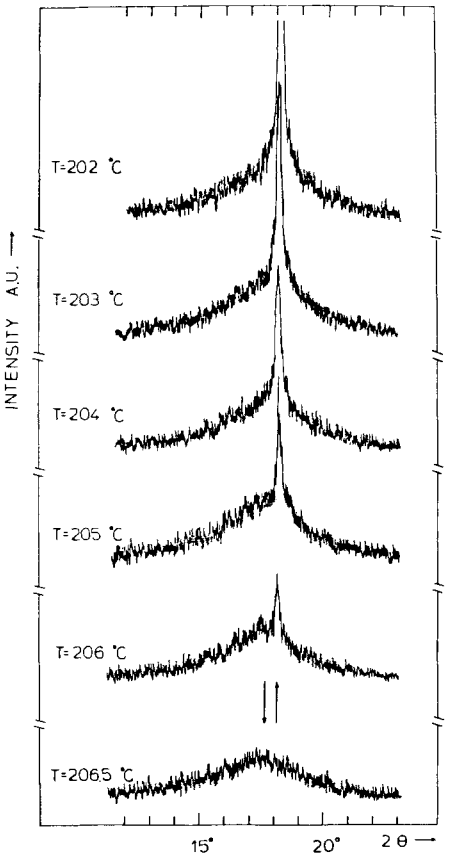

FIGURE 5 X-ray intensity *versus* diffraction angle 2Θ for different values of temperature in relation to the S_B–N phase transition.

Figure 5 shows the diffraction pattern obtained at the smectic B–nematic phase transition by heating the sample. An interesting phase coexistence also appears at this transition. As the temperature is increased, the intensity of the 100 peak characteristic of the smectic B phase,[9-10] progressively decreases, whereas the diffuse peak associated with the nematic phase progressively grows, changing in its form until the characteristic profile of a nematic phase is reached. The arrows in Figure 5 emphasize the shift of the peaks corresponding to the two phases.

3. DISCUSSION

The most important aspect of the crystal structure of the phase stable at room temperature is the dimeric organization of the molecules held together by hydrogen bonds. A similar dimeric arrangement of the structural repeating unit is retained in the smectic B phase of this compound.[7] Actually an interlayer distance $d_{001} = 35.0 \pm 0.4$ Å was obtained for this phase.[7]

This value agrees with that obtained from the dimer length of 30.25 Å, taken as the distance between the two extreme methyl groups of the dimer, as found in the K_2 phase, increased by the Van der Waals distance between these groups of about 4 Å.

Whereas in the K_2 solid phase, the dimers are inclined to the (100) plane with an interlayer distance of 21.75 Å, in the smectic B phase the dimers are perpendicular to the (001) smectic planes.

From Figure 3 it appears that the low angle peak positions, corresponding to the interlayer spacing, are identical in the two K_1 and K_2 phases. This suggests that the dimeric organization, and in particular the tilt angle of about 40°, does not change on going over from the K_2 to the K_1 phase.

The disappearance of the dimer inclination in the smectic B phase is directly evident from Figure 4, as the 001 smectic B peak occurs at a lower angular position as compared with the corresponding peak for the K_1 phase. Moreover, the first order character of the transition appears from the abrupt change of the dimer tilt angle.

The intermolecular spacing $d_{100} = 4.87 \pm 0.04$ Å is obtained from the position of the sharp peak of the smectic B phase shown in Figure 5. Hence the interplanar distance in a pseudo-hexagonal arrangement is equal to 5.62 ± 0.05 Å, in agreement with the results of reference 7. By using the modified Bragg law[11]

$$1.117\lambda = 2d \sin\theta$$

where λ is the X-ray wavelength and 2θ is the angular position of the broad peak corresponding to the nematic phase, a value of 5.67 ± 0.06 Å is obtained for the intermolecular distance. This value practically coincides with that obtained for the smectic B phase and is in agreement with the average hindrance of the dimer deduced from the molecular structure.

Acknowledgments

We thank Prof. B. Samorì for helpful advice and discussion, the Istituto di Chimica Generale, Università di Parma for collection of the X-ray intensity data, and C.N.R. (Roma) for financial support. Moreover the valuable technical assistance of Mr. R. Bartolucci and S. Polenta is gratefully acknowledged.

References

1. D. E. Martire in "*The Molecular Physics of Liquid Crystals*," (G. R. Luckhurst and G. W. Gray Eds.), Academic Press, London, 1979, Chap. 11.
2. M. D. Croucher and D. Patterson, *J. Chem. Soc. Faraday Trans. 1*, **77**, 1237 (1981).
3. G. F. Pedulli, C. Zannoni, and A. Alberti, *J. Magn. Res.*, **10**, 372 (1973).
4. B. Samorì, *J. Phys. Chem.*, **83**, 375 (1979).
5. B. Samorì and L. Fiocco, *J. Amer. Chem. Soc.*, **104**, 2634 (1982).
6. G. Albertini, A. Lodi, G. Poeti, F. Rustichelli, B. Samorì, and G. Torquati, *Nuovo Cimento Soc. Ital. Fis. B.*, in press.
7. S. Melone, V. Mosini, R. Nicoletti, B. Samorì, and G. Torquati, *Mol. Cryst., Liq. Cryst.*, in press.
8. G. M. Sheldrick, SHELX 75 System of Computer Programs, Cambridge (1975).
9. J. Doucet, A. M. Levelut, M. Lambert, L. Liebert, and L. Strzelecki, *J. Phys. Colloq.* (Orsay, Fr.), **36**, C1-3 (1975).
10. L. V. Azaroff, *Mol. Cryst., Liq. Cryst.*, **60**, 73 (1980).
11. A. De Vries, *Mol. Cryst., Liq. Cryst.*, **20**, 119 (1983).
12. G. Albertini, B. Dubini, S. Melone, M. G. Ponzi-Bossi, F. Rustichelli, and G. Torquati, *J. Phys.* (*Paris*), Colloque C3, 384 (1979).
13. A. Torgalkar, R. S. Porter, E. M. Barral II, and J. F. Johnson, *J. Chem. Phys.*, **48**, 3897 (1968).
14. J. Frenkel, "*Kinetic Theory of Liquids*," Dover Publications, Inc., New York, 1956.